Article

Not peer-reviewed version

The Utility of Mitochondria Detection Methods Applied as an Additional Tool for the Differentiation of Renal Cell Tumours

Gorana Nikolic *, Maja Zivotic *, Sanja Cirovic, Sanja Despotovic, Sanja Radojevic Skodric

Posted Date: 25 April 2023

doi: 10.20944/preprints202304.0879.v1

Keywords: renal cell tumours; renal cell carcinomas; immunohistochemistry; immunofluorescence; mitochondria; electron microscopy

Article

The Utility of Mitochondria Detection Methods Applied as an Additional Tool for the Differentiation of Renal Cell Tumours

Gorana Nikolic [1,*,†], Maja Zivotic [1,*,†], Sanja Cirovic [1], Sanja Despotovic [2] and Sanja Radojevic Skodric [1]

[1] Institute of Pathology, Faculty of Medicine University of Belgrade, Belgrade, Serbia
[2] Institute for Histology and Embryology "Aleksandar Đ. Kostić", Faculty of Medicine, University of Belgrade, Belgrade, Serbia
* Correspondence: gorana.nikolic@med.bg.ac.rs (G.N.); maja.zivotic@med.bg.ac.rs (M.Z.)
† These authors contributed equally to this work.

Abstract: The precise differentiation of renal cell tumours (RCTs) is sometimes hard to achieve using standard imaging and histopathological methods. This study investigated 43 cell renal cell carcinomas (ccRCC), 15 papillary renal cell carcinomas (pRCC), 20 chromophobe renal cell carcinomas (chRCC), and 18 renal oncocytomas (RO), stained with anti-mitochondria antibody (Thermo Scientific) by immunohistochemistry and immunofluorescence, and assessed by electron microscopy, in order to define mitochondria distribution pattern (coarse scanty, moderate granular and diffuse granular). Thus, the majority of males had coarse granular staining in the tumours, while females were almost equally distributed among groups ($p=0.005$). An average patient age, tumour side and dimension, and tumour stage were similar in all staining pattern groups. However, pathohistological tumour types had significantly different expression patterns, with the lower amount of staining detected in majority of ccRCC, moderate expression in all chRCC, and diffuse expression in all RO, pRCC and two cases of ccRCC ($p<0.001$) presented with higher nuclear grade ($p=0.005$). Moreover, with increased distribution of mitochondria, the intensity of staining was higher ($p<0.001$). Here we present a strategy that utilizes mitochondria detection to differentiate RO from chRCC, as well as to distinguish other frequent RCTs, such as ccRCC and pRCC.

Keywords: renal cell tumours; renal cell carcinomas; immunohistochemistry; immunofluorescence; mitochondria; electron microscopy

1. Introduction

The World Health Organization (WHO) in 2022 proposed a new classification of adult renal cell tumours, based on their histological findings, immunophenotypes, molecular findings and patients' outcomes [1]. The most common types of renal tumours are clear cell renal cell carcinoma (ccRCC), papillary renal cell carcinoma (pRCC), chromophobe renal cell carcinoma (chRCC) and renal oncocytoma (RO). The diagnosis of two specific subtypes, renal oncocytomas (RO) and chromophobe renal cell carcinoma (chRCC), however, remains a challenge due to overlapping histopathological features and the same origin [2]. Namely, the differentiation between chRCC and RO, on standard hematoxylin and eosin-stained section, is particularly difficult and often requires ancillary studies. In addition to RO and chRCC, a category of 'other oncocytic tumours' has been introduced, that represents a heterogeneous tumour group not classifiable as aforementioned entities or other tumour types with eosinophilic features. These entities are not specific and requires a wide spectrum of additional researches, representing primarily a clinical management tumour category rather than specific pathohistological diagnosis [3].

Different immunohistochemical stains have been used to differentiate kidney tumours. It is known that both cytokeratin (CK) and vimentin are positive in ccRCC and pRCC, while vimentin is negative in chRCC and RO. Furthermore, beside CK and vimentin, CK7 is positive in pRCC, in chRCC, as well as ccRCC with papillary features. RO shows absent or focal positivity of CK7.

 doi:10.20944/preprints202304.0879.v1

Although CK7 positivity in most of the cases distinguish chRCC from RO, studies showed that eosinophilic variant of chRCC overlaps with RO in expression of CK7 [4] especially on needle biopsies [5,6]. Another useful antibody that has been frequently used over the past two decades and appear to be useful in differential diagnosis of kidney tumours is anti-mitochondrial antibody, especially if molecular analyses are not available. Distribution of anti-mitochondrial staining in ccRCC could be granular but scanty, while immunoexpression in pRCC is intense, coarsely granular and diffuse. Immunoexpression in most RO show intense, diffuse, granular staining compared with perinuclear staining pattern in chRCC [7,8].

Beside immunohistochemical staining, transmission electron microscopy (TEM) provides valuable ultrastructural information in kidney tumours differentiation, especially distinction of RO and chRCC [9,10]. The tumour is considered as RO if tumour cells contain abundant mitochondria with lamellar cristae, occupying the whole cytoplasm. Most prominent TEM features of chRCC are multiple membrane-bound microvesicles, and less prominent mitochondria containing tubular cristae which are dominantly perinuclearly positioned, compared to RO [11]. pRCC is also analyzed by TEM showing numerous mitochondria [12]. Nevertheless, ccRCC explored by TEM revealed few mitochondria per cell or even a complete absence [13].

As known, immunofluorescence is widely routinely utilized for the evaluation of non-tumour kidney diseases, both on frozen and paraffin-embedded tissue [14,15]. However, its possibilities are not fully explored in the kidney tumour diagnosis. Considering that the most prominent ultrastructural differences between the most common types of renal cell tumours relay on the abundance and distribution pattern of mitochondria explored by TEM, our aim was to investigate whether immunohistochemistry and immunofluorescence by applying anti-mitochondria antibodies could be used as an additional techniques for adequate diagnosis of these renal tumours.

2. Materials and Methods

2.1. Tissue samples

The current study included 96 patients diagnosed with renal cell tumours. Among them, 43 samples belonged to clear cell renal cell carcinoma (ccRCC), 15 samples were diagnosed as papillary renal cell carcinoma (pRCC), 20 samples as chromophobe renal cell carcinoma (chRCC), and 18 cases of renal oncocytoma (RO). All diagnoses were reviewed by two experienced uropathologists and were based on hematoxylin and eosin (H&E), histochemical (HC) and immunohistochemical (IHC) slides using light microscopy (LM). All kidney samples, using aforementioned analyses, were explored on slides from formalin-fixed paraffin embedded (FFPE) blocks, and contained tumour and adjacent non-tumour kidney parenchyma. The material was collected from the archive of Pathology Department, Clinic of Urology, University Clinical Center of Serbia, Belgrade. The Ethic Committee of the Clinic of Urology of Clinical Center of Serbia granted approval to collect the samples from the archive, and carry out the study (Application Ref: 0152/20, dated March 4th, 2020). The study presented here was conducted following all ethical standards laid down in the 1964 Declaration of Helsinki. Since the study was carried out retrospectively, according to our ethical issues, informed consents of patients were not required.

2.2. Clinical patients' data and gross tumour examination

All used clinical patient data (gender, age, tumour side) and data obtained during gross pathohistological examination (tumour dimensions), were collected from medical records and pathohistological reports.

2.3. Routine light microscopy tissue analyses

Paraffin blocks were cut into 4 μm thick sections, and afterwards stained routinely with H&E. Depending on the tumour morphology and differential diagnosis, additional HC (Halle colloid iron) and/or IHC (CAIX, CK7, CD117, CD10, vimentin, AMACR, RCC) were performed in order to get

 doi:10.20944/preprints202304.0879.v1

final pathohistological diagnosis. Slides were analyzed using Olympus BX51 light microscope, Olympus C5060A-ADU digital camera, and analySIS 5.0 software (Soft Imaging System, Olympus).

2.4. Immunohistochemical staining and analysis

All kidney samples were selected and IHC stained with mouse Mitochondria antibody Ab-2 (clone MTC02, Thermo Scientific, dilution 1:100). Tumour sections (4 μm thick) were deparaffinized and rehydrated. For the antigen retrieval, we used citrate buffer (pH 6.0, 20 minutes in the microwave). Primary antibody was incubated for 1h at room temperature. Sections were then treated with EnVision™ Detection System (DAKO, Germany), using 3,3'-diaminobenzidine or 3-amino-9-ethyl carbazole as substrate and counterstained with hematoxylin. Negative controls were performed by omitting the first antibody and stained by the EnVision™ method. Two pathologists reviewed all slides for the presence or absence of mitochondria expression in tumour samples. The slides were evaluated using Olympus BX51 light microscope, Olympus C5060A-ADU digital camera, and analySIS 5.0 software (Soft Imaging System, Olympus.

2.5. Immunofluorescence staining and analysis

The same FFPE specimens that were stained by IHC with mouse mitochondria antibody Ab-2 were also used in the IF analysis in order to determine the sensitivity of the above mentioned IHC antibody. For that purpose, 4 μm-thick FFPE sections were treated as previously described [16]. The FFPE sections were then proceeded to antigen retrival procedure applying citrate buffer of pH 6.0, as described in the IHC analysis section (20 min). Afterwards, the slides were incubated overnight with the primary mouse monoclonal mitochondria antibody Ab-2 (Clone MTC02, Thermo Scientific, dilution 1:100), followed by the secondary goat anti-mouse IgG-Alexa 488 (diluted 1:1000, Invitrogen) for 45 min at room temperature. The cell nuclei were identified by counterstaining with 4,6-diamino-2-phenylindolyldihydrochloride (DAPI; 1 μg/ml Sigma-Aldrich, Germany). Negative controls were performed in all experiments by omitting the first antibody. In each staining experiment, cross-binding of the secondary fluorescence labeled antibody was controlled on specific control slides on which the first and/ or second antibody was omitted. Tissue sections were mounted with Fluoro Preserve Reagent (Calboichem, Germany). All the slides were analyzed by epifluorescence microscopy using F-View-CCD camera (Olympus BX53, Germany). For the specific antibody staining, digital pictures from each fluorescence channel were taken and superimposed, using the software Solo Imaging Systems (Bioview, Israel).

2.6. Transmission electron microscopy

For transmission electron microscopy (TEM) analysis, paraffin blocks with kidney samples were cut into smaller pieces, approximately 2x2 mm in size, deparaffinized in xylol (2 minutes, four times), rehydrated in graded ethanol (100%- 2 changes, 96%, 70%, 50%, each change 5 minutes) to distillated water and rinse in phosphate buffer solution for 5 minutes. The samples were re-fixed in 3% glutaraldehyde in cacodylate buffer, post fixed in 1% OsO4 and 4,8% uranyl-acetate, dehydrated in graded ethanol and embedded in Epoxy medium, according to standard procedure [17]. The ultrathin sections were stained with uranyl acetate and lead citrate and examined with a Transmission Electron Microscope (TEM) (Morgagni 268D FEI, Hillsboro, OR, USA).

3. Results

3.1. Expression pattern of anti-mitochondria antibody in renal cell tumours - description of patient cohort

The study included 96 patients diagnosed with the most frequently pathohistological types of renal cell tumours. Their clinical and pathohistological characteristics were analyzed in three different groups, based on the IHC staining pattern of anti-mitochondria antibody (Table 1). Staining patterns were defined as coarse scanty, moderate granular and diffuse granular cytoplasmic staining. The majority of males (51.9%) had coarse scanty cytoplasmic staining, while females had similar

Preprints (www.preprints.org) | NOT PEER-REVIEWED | Posted: 25 April 2023 doi:10.20944/preprints202304.0879.v1

distribution in all three groups of staining patterns (Table 1). Patients were in similar ages in all groups (mean values around 60 years), without significant difference (Table 1). Renal cell tumours were surgically removed from both left and right kidneys, and the tumour side did not influence staining pattern, as shown in Table 1. Similarly, the average values of the largest tumour dimensions were not statistically different within the groups, and were usually around 60 mm (Table 1). The largest tumour was diagnosed as ccRCC with the maximal dimension of 200 mm, and the smallest one, also diagnosed as ccRCC, had 13 mm in the largest diameter. Statistically significant different expression pattern was observed in various pathohistological renal cell tumour types (Table 1). Among them, ccRCC was mostly diagnosed with the least amount of mitochondria detected by IHC, with exception of two cases found with diffuse granular staining pattern. All pRCC and RO were found with diffuse granular cytoplasmic staining, while chRCC was exclusively diagnosed with moderate granular staining. These differences among pathohistological types were statistically significant ($p<0.001$). With regard to two ccRCC cases, described with a diffuse granular mitochondrial staining, both were with higher nuclear grade ($p=0.005$), as shown in Table1. Staging of tumour disease were also explored in relation to the expression patterns of mitochondrial IHC staining (Table 1), however, the significant difference was not observed ($p=0.764$). Overall, it has been noticed that IHC staining intensity was increased in groups moderate and diffuse granular pattern ($p<0.001$), as presented in Table 1.

Table 1. Clinical and pathological characteristics of patents' cohort among three different mitochondria staining patterns.

Clinical and pathological characteristics		**Distribution pattern of mitochondria staining**			*p*
		Coarse scanty	**Moderate granular**	**Diffuse granular**	
Gender	*male*	28 (51.9 %)	5 (9.3 %)	21 (38.9 %)	p=0.005
n (%)	*female*	13 (31.0%)	15 (35.7 %)	14 (33.3 %)	
Age (average age ± SD)		60.9 ± 9.0	61.6 ± 8.3	61.2 ± 10.3	p=0.960
Side	*left*	23 (43.4 %)	9 (17.0 %)	21 (39.6%)	p=0.478
n (%)	*right*	17 (41.5 %)	11 (26.8%)	13 (31.7%)	
Highest tumour dimension (average mm ± SD)		64.8 ± 36.5	59.8 ±26.2	63.9 ± 34.2	p=0.865
Tumour type	*Clear cell RCC*	41 (95.3 %)	0 (0.0 %)	2 (4.7 %)	p<0.001
n (%)	*Papillary RCC*	0 (0.0 %)	0 (0.0 %)	15 (100 %)	
	Chromophobe RCC	0 (0.0 %)	20 (100 %)	0 (0.0 %)	
	Oncocytoma	0 (0.0 %)	0 (0.0 %)	18 (100 %)	
Nuclear grade- ccRCC	*Low grade (NG I. II)*	30 (100 %)	0 (0.0%)	0 (0.0%)	p=0.005
n (%)	*High grade (NG III. IV)*	11 (84.6 %)	0 (0.0%)	2 (15.4 %)	
T staging	*T1a*	8 (44.4 %)	4 (22.2 %)	6 (33.3 %)	p=0.764
n (%)	*T1b*	20 (71.4 %)	7 (25.0 %)	1 (3.6 %)	
	T2a	5 (35.7 %)	5 (35.7 %)	4 (28.6 %)	
	T2b	0 (0.0%)	1 (50.0 %)	1 (50.0%)	
	T3a	6 (50.0 %)	3 (25.0 %)	3 (25.0 %)	
	T3b	1 (100.0 %)	0 (0.0%)	0 (0.0%)	
	T4	1 (100.0 %)	0 (0.0%)	0 (0.0%)	
Expression intensity of anti-mitochondrial antibody	*mild to moderate*	41 (95.3 %)	0 (0.0%)	2 (4.7 %)	p<0.001
	strong	0 (0.0%)	20 (37.7 %)	33 (62.3 %)	

Preprints (www.preprints.org) | NOT PEER-REVIEWED | Posted: 25 April 2023 doi:10.20944/preprints202304.0879.v1

3.2. Visualization of mitochondria in non-tumour kidney samples

Applying immunohistochemistry and immunofluorescence, in the non-tumour adjacent kidney parenchyma, mitochondria were detected both in proximal and distal tubules, showing variable intense granular staining pattern with anti-mitochondria antibody, while glomeruli were completely negative (Figure 1A-B).

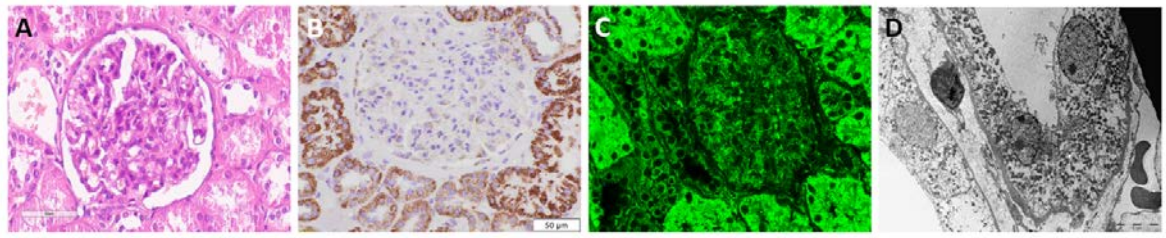

.

Figure 1. Mitochondria visualization in normal kidney and renal cell tumours. (**A**) IHC and (**B**) IF microphotograph of mitochondria distribution in normal human kidney; (**C**) IHC and (**D**) IF images of ccRCC; (**E**) IHC and (**F**) IF images of pRCC; (**G**) IHC and (**H**) IF images of chRCC; (**I**) IHC and (**J**) IF images of RO.

3.3. Clear cell renal cell carcinoma - ccRCC

Using anti-mitochondria antibody, coarse scanty granular IHC staining was visible in the majority of ccRCC. Detected granules were dispersed and randomly distributed (Figure 1C). Similarly, applying immunofluorescence, very weak signals were detected on IF images (Figure 1D). Nevertheless, morphologically ccRCC with lower nuclear grade and clear cytoplasm (Figure 2A) exhibited less, and even few, mitochondria detected by TEM (Figure 2B-C), compared to ccRCC with higher nuclear grade and slightly eosinophilic cytoplasm (Figure 2D) which showed increased number of mitochondria (Figure 2E-F).

3.4. Papillary renal cell carcinoma - pRCC

All pRCC samples expressed diffuse disperse granular IHC staining patterns, and depending on the morphology (low/high grade pRCC) had diffuse uniform pattern throughout the whole cytoplasm (low grade) or intense granular pattern apically accentuated (high grade). Figure 1E illustrates low grade pRCC IHC staining pattern with uniform diffuse disperse granular distribution, and similar appearance on IF images (Figure 1F). Morphologically, eosinophilic cells visible on optical microscopy (Figure 2G), have shown prominent, tightly packed mitochondria on EM analysis (Figure 2H-I).

3.5. Chromophobe renal cell carcinoma - chRCC

The IHC analysis of chRCC showed course granular cytoplasmic staining, localized mostly along the cell membrane. Some dispersed granular staining was detected in cytoplasm, but an areas around nuclei remained unstained, illustrating a prominent perinuclear halo (Figure 1G). Numerous granules were also detected by IF with heterogeneous IF signal intensity, but to a lesser extent compared to IHC staining (Figure 1H). Scattered mitochondria were predominantly localized on the periphery of the cell (along the cell membrane), but were in general with a moderate granular staining pattern. A prominent cell membranes visible morphologically (Figure 2J) and distribution of mitochondria were confirmed by EM (Figure 2K-L). All diagnostic approaches, including IHC, IF and EM analyses enables detection of some intracytoplasmic microvesicles of unknown origin, specifically found in chRCC.

Preprints (www.preprints.org) | NOT PEER-REVIEWED | Posted: 25 April 2023 doi:10.20944/preprints202304.0879.v1

3.6. Renal oncocytoma - RO

Contrary to the anti-mitochondria IHC staining of ccRCC, pRCC and chRCC, the staining in RO was the most intensive, diffuse and finely granular (Figure 1I). The same pattern was confirmed by IF staining (Figure 1J). Bearing in mind that electron microscopy confirmed that RO is rich in mitochondria (Figure 2N-O), our immunostaining analyses, both IF and IHC, verified that anti-mitochondria staining could be specific and sensitive for RO. Furthermore, it was also confirmed that "oncocytic" cell morphology (Figure 2M) was a clear consequence of numerous mitochondria diffusely localized within the cytoplasm.

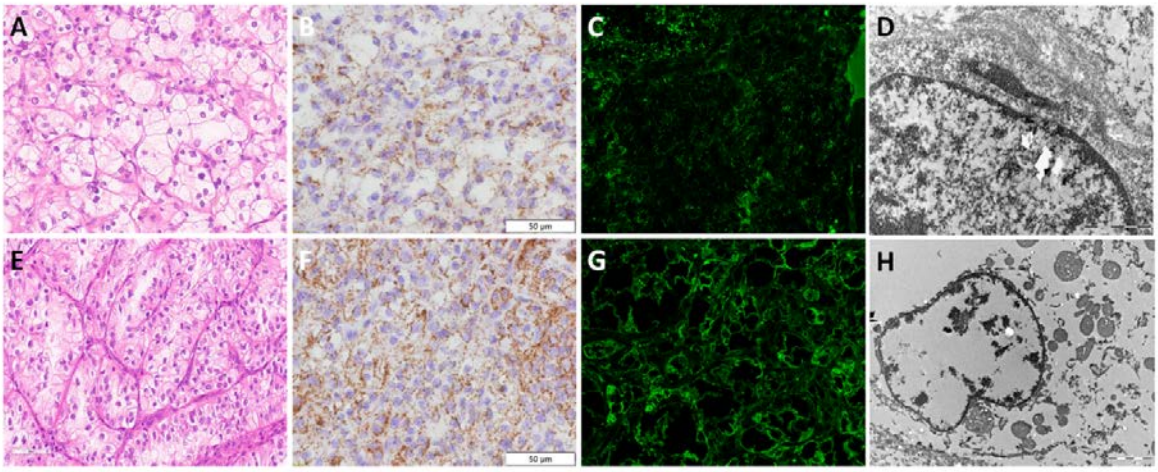

Figure 2. Morphology and mitochondria visualization by transmission electron microscopy in renal cell tumours. (**A**) H&E and (**B-C**) TEM microphotograph of mitochondria distribution in ccRCC (lower nuclear grade); (**D**) H&E and (**E-F**) TEM microphotograph of mitochondria distribution in ccRCC (higher nuclear grade); (**G**) H&E and (**H-I**) TEM microphotograph of mitochondria distribution in pRCC; (**J**) H&E and (**K-L**) TEM microphotograph of mitochondria distribution in chRCC; (**M**) H&E and (**N-O**) TEM microphotograph of mitochondria distribution in RO.

4. Discussion

It is well known that classic ccRCC and pRCC have specific morphological features enabling easier distinguishing. The main challenges still remain regarding the eosinophilic variants of RCT due to their morphological overlaps, especially using only H&E slides. Therefore, additional diagnostic methods, such as IHC, HC staining, TEM and molecular profiling, are in use. Beside the fact that these methods are time-consuming and require different tissue fixation, they also have additional limitations.

Considering that the quality of FFPE slides IHC staining highly depends on the adequacy of preanalytical phase, such as tissue fixation procedures, as well as on the establishment of staining protocol, balancing between peroxidase and protein blockade, antigen retrival procedures, antibody clones and their dilutions, visualization of antigen-antibody reactions, thus, the results of IHC staining and their interpretations could be sometimes hard for pathologists [18,19]. Especially, when highly specialized patholohistological laboratories receive a samples previously fixed and paraffin-embedded in other institutions, there is no a single way to standardize and establish the unique protocols [19]. Due to non-standardized and variably FFPE tissue preparation among laboratories such as different fixative solutions, duration of paraffin baths ect, further microscopic slides staining procedures could lead to false negativity or even unspecific positivity of IHC [19]. For example, also HC staining such as Hale's colloidal iron, frequently used for differentiation between RO and chRCC, fails to stain adequately [11,20]. Moreover, renal neoplasms with focal mucin-like changes, such as oncocytomas and papillary renal neoplasms, could be mildly to moderately stained with Hale's colloidal iron. Thus, RCT with extensive chromophobe cell-like features may pose a differential diagnostic problem with chRCC when pathohistological examination is based on the HC staining [21]. In that case, TEM is a gold standard for distinguishing these types of tumours. For example,

tumour cells of RO are filled with uniform and round mitochondria. They are closely packed in the cytoplasm and their size is larger than those in chRCC. Beside mitochondria, scattered microvesicles are also present and their number varies from cell to cell. They are either absent or very sparse, contrary to chRCC. In chRCC, the number and shape of mitochondria depends on the number of microvesicles. Their distribution can be diffuse or localized in the peripheral cytoplasm [22,23]. However, TEM is not in widely use for daily practice, considering requirements of specially trained human resources (technicians and pathologists), along with the expensive equipment and high depreciation costs [23]. It is also important to use an adequate fixation procedure for TEM, since all required fine ultrastructural details such as mitochondria cristae and microvesicles could not be interpreted on TEM slides form FFPE tissues, as we noticed in our results. Here, we were only able to detected mictrochonria presence, their number, localization and shape, but we could not see all these important details of their structure, as authors found in RCTs properly fixed for TEM analysis [12]. Indeed, in order to use TEM for diagnostic purpose in uropathology, a piece of kidney tumor samples should be stored in adequate fixative.

Beside standard H&E and HC slides, routinely used wide panel spectrum of IHC antibodies and TEM analyses, authors explored also the utility of different mitochondria antibodies, considering that the main ultrastructural differentiation of RTCs is based on this cellular organelle differences in major RCT types. Therefore, Mete *et al.* used anti-mitochondria (AMA- NeoMarkers) antibody, and the pattern of immunoreactivity was mostly diffuse in RO, while diffuse, but peripherally accentuated in the most chRCCs, thus, they proposed very high sensitivity (96%) and specificity (94%) of AMA staining for differentiation of chRCCs from ROs [7]. Similarly, Kuroda *et al.* detected mitochondria by MIA-Biogenex and showed strong and diffuse positivity in oncocytic chRCC, without description of the staining pattern [8]. With the same regard, Tickoo *et al*. described diffuse and fine granular positivity of antimitochondrial antibody 113-1 in all examined ROs and peripheral accentuation of coarse cytoplasmic granules in chRCCs. Other eosinophilic and granular type of tumours mostly showed irregular coarsely granular and diffuse staining [24]. In our study, we used mitochondrial antibody (MA-Thermofischer) and obtained diffuse intensive fine granular cytoplasmic staining in RO, and intensive with coarse granularity and mostly periphery localized staining among chRCC. In ccRCC, cytoplasmic staining was coarse scanty granular cytoplasmic in the most cases. However, we also detected the ccRCCs with higher nuclear grade and with eosinophilic cytoplasm with increased mitochondria expression. All pRCC samples expressed diffuse disperse granular IHC staining patterns, and depending on the morphology (low/high grade pRCC) had diffuse uniform pattern throughout the whole cytoplasm (low grade) or intense granular pattern apically accentuated (high grade). Our results are in accordance with the literature data, so regardless of the clone that is in use, the mitochondrial antibody can be included in standard IHC panel for renal neoplasms, since it could provide additional hints for the precise diagnosis.

Although IF analysis is not widely in use in routine diagnostics of renal neoplasms, here we showed an agreement of IF results with the results obtained by IHC, and all these results correlated with the TEM visualized mitochondria. The evaluation of immunofluorescence images requires expertise but trainee does not require much time [25]. Moreover, the standard H&E *ex tempore* pathohistological examination could not be always accurate and precise, considering that fresh-frozen tissue samples do not have preserved morphology. However, this type of unfixed fresh-frozen tissue sample allows high sensitivity of IF staining procedures [26], leading to fast and precise identification of mitochondria, therefore enabling establishment of precise diagnosis.

5. Conclusions

The application of immunostaining, especially immunofluorescence, using anti-mitochondria antibody can assist in fast and easy distinction of renal oncocytoma from chromophobe renal cell carcinoma and other eosinophilic variants of RCC with the high accuracy. Therefore, it can be used as an additional tool when diagnosis needs to be set quickly, mainly during preoperative and intraoperative fast decision in choosing the best surgical protocol for the patient, balancing between benefits from total or partial nephrectomy.

Author Contributions: conceptualization: GN and MZ.; methodology. G.N.; formal analysis. G.N, M.Z.; investigation. G.N., M.Z., S.C, S.D.; data curation. G.N., M.Z., S.C, S.D.; writing—original draft preparation. G.N., M.Z., S.C, S.D.; writing—review and editing. S.R.S.; visualization. S.R.S.; supervision. S.R.S.; funding acquisition. S.R.S. All authors have read and agreed to the published version of the manuscript.

Funding: This research was funded by the Ministry of Education, Science, and Technological Development of the Republic of Serbia (project Nos. III41006, MPN 175059).

Institutional Review Board Statement: The study was conducted in accordance with the Declaration of Helsinki and approved by the Professional Board of the Clinic for Urology, Clinical Centre of Serbia (protocol code 0152, 04/03/20) for studies involving human tissues.

Informed Consent Statement: Patient consent was waived because according to the policy of our Ethics Committee it is not required for retrospective studies, especially considering that the material used in this study was collected from the archive after diagnostic work was completed.

Data Availability Statement: All data are provided within the manuscript.

Acknowledgments: Miloš Kiš and Dragan Bešević (Institute of Histology and embryology, Faculty of Medicine, Belgrade) for excellent technical assistance with transmission electron microscopy. This work was supported by the Ministry of Education, Science, and Technological Development of the Republic of Serbia (projects No. III41006, MPN 175059).

Conflicts of Interest: The authors declare no conflict of interest. The funders had no role in the design of the study, in the collection, analyses or interpretation of data, in the writing of the manuscript or in the decision to publish the results.

References

1. Moch H; Amin M.B; Berney D.M; Compérat E.M; Gill A.J; Hartmann A; Menon S; Raspollini M.R; Rubin M.A; Srigley J.R; Hoon Tan P; Tickoo S.K; Tsuzuki T; Turajlic S; Cree I; Netto G.J. The 2022 World Health Organization Classification of Tumours of the Urinary System and Male Genital Organs-Part A: Renal, Penile, and Testicular Tumours. *Eur Urol*. **2022**, 82, 458-468. doi: 10.1016/j.eururo.2022.06.016.
2. Störkel S; Steart P.V; Drenckhahn D; Thoenes W. The human chromophobe cell renal carcinoma: its probable relation to intercalated cells of the collecting duct. *Virchows Arch B Cell Pathol Incl Mol Pathol*. **1989**, *56*, 237-45. doi: 10.1007/BF02890022.
3. Trpkov K; Hes O; Williamson S.R; Adeniran AJ; Agaimy A; Alaghehbandan R; Amin M.B; Argani P; Chen Y.B; Cheng L; Epstein J.I; Cheville J.C; Comperat E; da Cunha I.W; Gordetsky J.B; Gupta S; He H; Hirsch M.S; Humphrey P.A; Kapur P; Kojima F; Lopez J.I; Maclean F; Magi-Galluzzi C; McKenney J.K; Mehra R; Menon S; Netto G.J; Przybycin C.G; Rao P; Rao Q; Reuter V.E; Saleeb R.M; Shah R.B; Smith S.C; Tickoo S; Tretiakova M.S; True L; Verkarre V; Wobker S.E; Zhou M; Gill A.J. New developments in existing WHO entities and evolving molecular concepts: The Genitourinary Pathology Society (GUPS) update on renal neoplasia. *Mod Pathol*. **2021**, *34*, 1392-1424. doi: 10.1038/s41379-021-00779-w.
4. Liu Y.J; Ussakli C; Antic T; Liu Y; Wu Y; True L; Tretiakova MS. Sporadic oncocytic tumors with features intermediate between oncocytoma and chromophobe renal cell carcinoma: comprehensive clinicopathological and genomic profiling. *Hum Pathol*. **2020**, *104*, 18-29. doi: 10.1016/j.humpath.2020.07.003.
5. Wu A. Oncocytic Renal Neoplasms on Resections and Core Biopsies: Our Approach to This Challenging Differential Diagnosis. *Arch Pathol Lab Med*. **2017**, *141*, 1336-1341. doi: 10.5858/arpa.2017-0240-RA.
6. Williamson S.R; Gadde R; Trpkov K; Hirsch M.S; Srigley J.R; Reuter V.E; Cheng L; Kunju L.P; Barod R; Rogers C.G; Delahunt B; Hes O; Eble J.N; Zhou M; McKenney J.K; Martignoni G; Fleming S; Grignon D.J; Moch H; Gupta N.S. Diagnostic criteria for oncocytic renal neoplasms: a survey of urologic pathologists. *Hum Pathol.* **2017**, *63*, 149-156. doi: 10.1016/j.humpath.2017.03.004.
7. Mete O; Kilicaslan I; Gulluoglu M.G; Uysal V. Can renal oncocytoma be differentiated from its renal mimics? The utility of anti-mitochondrial, caveolin 1, CD63 and cytokeratin 14 antibodies in the differential diagnosis. *Virchows Arch*. **2005**, *44*, 938-46. doi: 10.1007/s00428-005-0048-6.
8. Kuroda N; Tanaka A; Yamaguchi T; Kasahara K; Naruse K; Yamada Y; Hatanaka K; Shinohara N; Nagashima Y; Mikami S; Oya M; Hamashima T; Michal M; Hes O. Chromophobe renal cell carcinoma, oncocytic variant: a proposal of a new variant giving a critical diagnostic pitfall in diagnosing renal oncocytic tumors. *Med Mol Morphol*. **2013,** *46*, 49-55. doi: 10.1007/s00795-012-0007-7.
9. Johnson N.B; Johnson M.M; Selig M.K; Nielsen GP. Use of electron microscopy in core biopsy diagnosis of oncocytic renal tumors. *Ultrastruct Pathol*. **2010**, *34*, 189-94. doi: 10.3109/01913121003725713.
10. Pusiol T; Franceschetti I; Scialpi M; Piscioli I; Tardio M.L. Electron microscopy: the gold standard in the differential diagnosis of chromophobe renal cell carcinoma and oncocytoma. *Anal Quant Cytol Histol*. **2010**, *32*, 58-60.
11. Abrahams N.A; MacLennan G.T; Khoury J.D; Ormsby A.H; Tamboli P; Doglioni C; Schumacher B; Tickoo S.K. Chromophobe renal cell carcinoma: a comparative study of histological, immunohistochemical and ultrastructural features using high throughput tissue microarray. *Histopathology*. **2004**, *45*, 593-602. doi: 10.1111/j.1365-2559.2004.02003. x.
12. Pradhan, D., Kakkar, N., Bal, A. *et al.* Sub-typing of renal cell tumours; contribution of ancillary techniques. *Diagn Pathol.* **2009**, *4*, 21. doi: 10.1186/1746-1596-4-21.
13. Nilsson, H., Lindgren, D., Mandahl Forsberg, A. *et al.* Primary clear cell renal carcinoma cells display minimal mitochondrial respiratory capacity resulting in pronounced sensitivity to glycolytic inhibition by 3-Bromopyruvate. *Cell Death Dis* 6. **2015**, e1585. doi: 10.1038/cddis.2014.545.
14. Messias N.C; Walker P.D; Larsen C.P. Paraffin immunofluorescence in the renal pathology laboratory: more than a salvage technique. *Mod Pathol*. **2015**, 28, 854-60. doi: 10.1038/modpathol.2015.1.
15. Nasr S.H; Fidler M.E; Said S.M. Paraffin Immunofluorescence: A Valuable Ancillary Technique in Renal Pathology. *Kidney Int Rep*. **2018,** *3*, 1260-1266. doi: 10.1016/j.ekir.2018.07.008.
16. Bosic M; Brasanac D; Stojkovic-Filipovic J; Zaletel I; Gardner J. Cirovic S. Expression of p300 and p300/CBP associated factor (PCAF) in actinic keratosis and squamous cell carcinoma of the skin. *Exp Mol Pathol*. **2016**, 100. doi: 10.1016/j.yexmp.2016.03.006.
17. Vujicic M; Saksida T; Despotovic S; Bajic S.S; Lalić I; Koprivica I; Gajic D; Golic N; Tolinacki M; Stojanovic I. The Role of Macrophage Migration Inhibitory Factor in the Function of Intestinal Barrier. *Sci Rep*. **2018**, *8*, 6337. doi: 10.1038/s41598-018-24706-3.
18. Kim S.W; Roh J; Park C.S. Immunohistochemistry for Pathologists: Protocols, Pitfalls, and Tips. *J Pathol Transl Med*. **2016**, 50(6):411-418. doi: 10.4132/jptm.2016.08.08.
19. Libard S; Cerjan D; Alafuzoff I. Characteristics of the tissue section that influence the staining outcome in immunohistochemistry. *Histochem Cell Biol.* **2019**, 151, 91–96. doi:10.1007/s00418-018-1742-1

20. Tickoo S.K; Lee M.W; Eble J.N; Amin M; Christopherson T; Zarbo R.J; Amin M.B. Ultrastructural observations on mitochondria and microvesicles in renal oncocytoma, chromophobe renal cell carcinoma, and eosinophilic variant of conventional (clear cell) renal cell carcinoma. *Am J Surg Patho*l. **2000**, 24, 1247-56. doi: 10.1097/00000478-200009000-00008
21. Mai K.T; Burns B. F. Chromophobe cell carcinoma and renal cell neoplasms with mucin-like changes. *Acta Histochemica;* ***2000***, 102, 103–113. doi:10.1078/0065-1281-00543
22. Yusenko M.V. Molecular pathology of chromophobe renal cell carcinoma: A review. *International Journal of Urology*. **2010**, 17: 592-600. doi:10.1111/j.1442-2042.2010.02558.x
23. Inkson, B.J. Scanning Electron Microscopy (SEM) and Transmission Electron Microscopy (TEM) for Materials Characterization. In *Book Title*: Materials Characterization Using Nondestructive Evaluation (NDE) Methods. **2016**, pp.17-43. doi:10.1016/B978-0-08-100040-3.00002-X.
24. Tickoo, S.K., Amin, M.B., Linden, M.D., Lee, M.W., & Zarbo, R.J. (1997). Antimitochondrial antibody (113-1) in the differential diagnosis of granular renal cell tumors. *The American journal of surgical pathology*. **1997**, *21 8*, 922-30.
25. Piña R; Santos-Díaz A.I; Orta-Salazar E; Aguilar-Vazquez A.R; Mantellero C.A; Acosta-Galeana I; Estrada-Mondragon A, Prior-Gonzalez M; Martinez-Cruz J.I; Rosas-Arellano A. Ten Approaches That Improve Immunostaining: A Review of the Latest Advances for the Optimization of Immunofluorescence. *Int J Mol Sci*. **2022**, 23, 1426. doi: 10.3390/ijms23031426.
26. Honvo-Houéto E; Truchet S. Indirect Immunofluorescence on Frozen Sections of Mouse Mammary Gland. *J Vis Exp*. **2015**, 106, 53179. doi: 10.3791/53179.